Quantum Chemical Determination of the Equilibrium Geometries and Harmonic Vibrational Frequencies of 1,1′-, 1,2′- and 2,2′-Binaphthyl in Their Ground and Excited (^1L_a) Electronic States

Fangtong Zhang, George B. Bacskay,* and Scott H. Kable

School of Chemistry, University of Sydney, New South Wales, 2006, Australia

Received: August 4, 2003; In Final Form: October 16, 2003

This work is concerned with the characterization of the lowest electronic excited states of 1,1′-, 1,2′- and 2,2′-binaphthyl, in particular with the determination of their equilibrium geometries, low-frequency vibrations, and torsional potentials, via ab initio and density functional (DFT) calculations. The methods employed are configuration interaction with singles (CIS) and time-dependent DFT, in conjunction with Hartree−Fock and DFT(B3LYP) theories for the ground states, using the 3-21G basis set. The strengths and weaknesses in these methods for these large systems were tested extensively by reference to higher level calculations performed on the benzene/biphenyl systems and on naphthalene itself. In the case of 1,2′- and 2,2′-binaphthyl the theoretical predictions are consistent with a reassignment of the experimentally observed spectrum as $S_3(^1L_a) \leftarrow S_0$ rather than $S_1(^1L_b) \leftarrow S_0$ as previously assumed. With this reassignment it is possible to provide definitive assignment of a number of the observed low-frequency torsional and out-of-plane bending modes, as well as a more confident identification of the conformation of the observed excited states. For 1,1′-binaphthyl the theoretical results are, however, at variance with the prevailing interpretation of the spectral data. As expected on the basis of qualitative π molecular orbital theory, π-delocalization has been found to be considerably more important in the ^1L_a excited states of the binaphthyls than in the ground and ^1L_b excited states. The different degrees of π delocalization in the ground and excited states of these biaryls provide an explanation as to why all these systems adopt nonplanar twisted geometries in their ground and ^1L_b excited states, while in their ^1L_a excited states they are computed to be either completely planar or considerably more so than in the ground state.

Introduction

The electronic spectroscopy and molecular structure of binaphthyl (BN) molecules, where two naphthalene rings are connected by a CC bond, have been the subject of numerous studies,[1−14] along with a range of other biaryl systems.[15−23] To date, most computational studies on biaryls have been carried out at a semiempirical level of theory,[24−29] although for biphenyl (BP) a number of ab initio and density functional calculations have been reported.[21,30,31] Much of the interest in both spectroscopic and theoretical studies has focused on the conformation of such systems, i.e., the magnitude of the dihedral (torsional) angle between the two aromatic rings, given that the associated torsional potential is affected by electronic π-delocalization (conjugation) and steric and environmental factors. For example, in 1,1′-binaphthyl (1,1′-BN), the two naphthalene rings are near-perpendicular to each other in both ground (S_0) and first excited singlet (S_1) states,[1−3,27] while in 2,2′-binaphthyl (2,2′-BN) the torsional angles are believed to be approximately 30°, 25°, 20°, and 0° in the $S_0(1^1A)$, $S_1(1^1B)$, $S_2(2^1A)$, and $S_3(2^1B)$ states, respectively.[13,29] These conformations are consistent with the relative degree of steric hindrance in these binaphthyls in their planar configurations as well as suggesting an increased degree of π conjugation in the S_3 state of 2,2′-BN. The structural formulas of the three BNs are shown in Figure 1, along with diagrams which provide a simple geometric classification of the steric interactions that occur in the BNs.

The room-temperature electronic absorption spectra of these large molecules are broad.[1] All three isomers have been investigated also in supersonic free jets. Jonkman and Wiersma studied 1,1′-BN some 20 years ago,[3,9] while 2,2′-BN and 1,2′-BN were examined more recently by Del Riccio et al. and Zhang et al.[13] Analysis of the LIF spectra yielded frequencies associated with the torsional modes of these molecules as well as estimates for the changes in torsional angles that occur on excitation.

In conjunction with the experimental investigation of Del Riccio et al.[13] and Zhang et al.[14] we also undertook a complementary quantum chemical study of the problem. Using methods based on ab initio and density functional theories, we set out to determine the equilibrium geometries and vibrational frequencies of all three, viz., 1,1′-, 1,2′-, and 2,2′-BNs, in both ground and lowest excited singlet states and to characterize their torsional potentials. In particular, we aimed at providing an assignment of the excited electronic states and identification of the low-frequency vibrational modes that had been observed.[13,14] Prior to this work only semiempirical studies had been carried out on these systems,[27−29] which focused on the torsional dependence of the ground and lowest four $^1(\pi\pi^*)$ excited states. While some of the results obtained appear to be consistent with experiment, discrepancies were also noted,[13,14] which, in part at least, provided the motivation to carry out higher level quantum chemical calculations utilizing ab initio and density functional methods.

In the interpretation of the LIF spectra of 1,2′- and 2,2′-BN,[13,14] it was assumed that the observed excited states

---

* Corresponding author. E-mail: g.bacskay@chem.usyd.edu.au.

10.1021/jp036271o CCC: $27.50

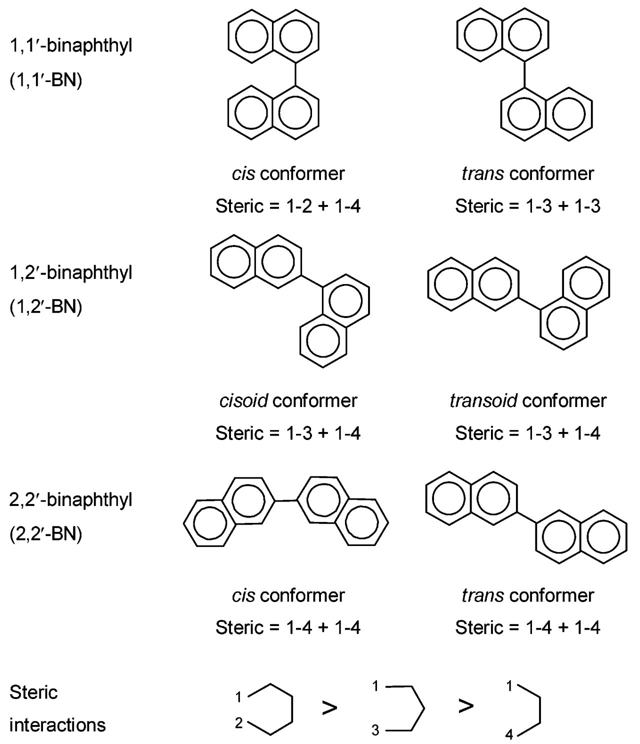

Figure 1. Structural formulas of the three binaphthyls. The general type of steric interactions that contribute to the torsional angle are shown at the bottom of each structure, with reference to the key at the bottom of the figure.

correspond to the S_1 states, which had been identified as ^1L_b states in the semiempirical studies of Baraldi et al.[28,29] and which correlate with the ^1L_b ($^1B_{2u}$) state of naphthalene. However, it is possible that the excited states in question are the ^1L_a states of these binaphthyls. The main thrust of the work reported here is to explore this possibility and thus carry out a detailed study of ^1L_a excited states, which correlate with the ^1L_a ($^1B_{1u}$) excited state of naphthalene. (The notation L_a, L_b was originally introduced by Platt[32] as a systematic way of classifying and correlating the excited states of cata-condensed aromatic hydrocarbons.) The work on BNs has been extended to include a comparative study of biphenyl (BP), which enables useful parallels to be drawn as well as identifying the differences between these two biaryl systems.

Theory and Computational Methods

The ground-state equilibrium geometries, force constants, and harmonic frequencies were determined at the Hartree−Fock SCF as well as density functional (DFT) levels of theory, utilizing the B3LYP functional, in conjunction with the split valence 3-21G basis set.

Analogous 3-21G geometry and frequency calculations were carried out for the appropriate excited states also, using the configuration interaction with single excitation (CIS) method[33] within the Hartree−Fock model. The adiabatic excitation energies and hence the 0−0 transition energies were recalculated by application of the potentially more accurate time-dependent DFT (TD-DFT) method,[34−37] using the B3LYP hybrid functional.

The 3-21G basis is regarded as the smallest that can be expected to yield sensible results as well as being affordable in terms of the computer resources for large molecules such as the BN systems. In a few selected calculations the 6-31G(d) basis was used so as to gauge the accuracy of the 3-21G results. These studies support our expectations that the key parameters of interest, viz., torsional angles and potentials, as well as the low-frequency vibrational modes, can be adequately described by the 3-21G basis.

The torsional potential energy surfaces in both ground and excited states were calculated at the B3LYP/3-21G and CIS/3-21G levels of theory, respectively. The strategy in these calculations was to allow full geometry relaxation at any fixed value of the torsional angle. Using the torsional potential energy surfaces that had been thus generated, the generalized finite element method (GFEM)[38] was used to solve the one-dimensional Schrödinger equation that yields torsional energy levels and Franck−Condon factors which are subject to the possible anharmonicity of the torsional potential.

As a test of the accuracy and reliability of the proposed methodology, a series of test calculations were carried out for the benzene, biphenyl, and naphthalene molecules using the larger 6-31G(d) basis as well as higher levels of theory, in particular the complete active space SCF (CASSCF)[39,40] and the complete active space second-order perturbation (CASPT2)[41,42] theories. This allows us to assess the performance of the CIS/3-21G and TD-B3LYP/3-21G methods for the prediction of geometries, frequencies, and excitation energies.

The quantum chemical calculations were carried out using the Gaussian98[43] and MOLCAS[44] programs on DEC alpha 600/5/333 and COMPAQ XP1000/500 workstations of the Theoretical Chemistry group at the University of Sydney and on the COMPAQ AlphaServer SC system of the Australian Partnership for Advanced Computing National Facility at the National Supercomputing Centre, ANU, Canberra.

Qualitative Molecular Orbital Description of Biaryls. The geometries, frequencies, and electronic excitation energies of biaryls, such as biphenyl and the binaphthyls studied in this work, are understood to be governed by two major effects: π-electron delocalization (conjugation) and steric interactions. While the former are maximized for a planar geometry, steric effects generally result in distortions from planarity, which are mostly torsional in character. Other effects, such as long-range electrostatic, polarization and dispersive interactions between the aryl moieties, i.e., the intramolecular analogues of the corresponding components of intermolecular forces, are expected to be less important.

As an aid to our understanding and appreciation of π-delocalization effects we found it useful to study biaryl systems, at least initially, in terms of a simple, qualitative π molecular orbital (MO) approach, such as Hückel theory.[45] While this is undoubtedly familiar territory to many readers, we hope that the majority of readers will derive some benefit from this simple preliminary analysis.

The results of Hückel calculations for BP and 2,2′-BN are shown in Figure 2. The pairwise interactions (as indicated by broken lines) of the benzene MO's result in nondegenerate pairs of b_{3u} and b_{2g} MO's for BP. The pairs of b_{1g} and a_u MO's arise as in- and out-of-phase combinations of one component of the e_{1g} or e_{2u} MO's of benzene. Due to the weak interactions, which in Hückel theory are actually zero, the resulting b_{1g} and a_u MO's are near-degenerate. The weaker interactions among the monomeric MO's with different energies result in further stabilization of the occupied b_{3u} and b_{2g} MO's of BP and a corresponding destabilization of the virtual b_{3u} and b_{2g} MO's. The net result of these weaker interactions according to Hückel theory is a lowering of the total π energy of BP by -0.38β (noting that $\beta < 0$). This is then a measure of the increased π-delocalization (conjugation) in the ground state. We note here that for BP

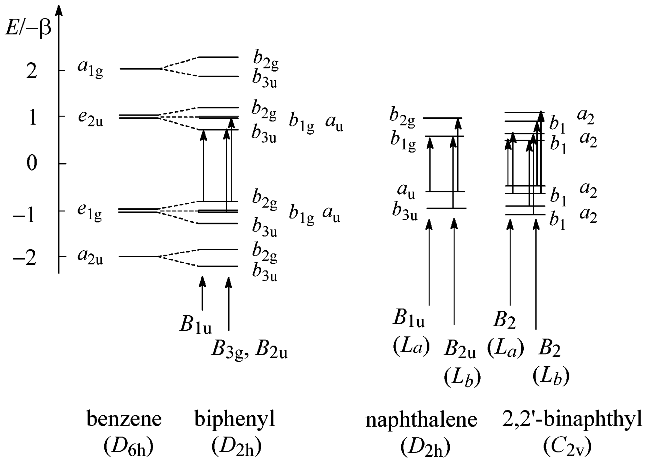

Figure 2. Correlation of benzene/biphenyl and naphthalene/2,2′-binaphthyl MO's.

essentially the same correlation diagram as that in Figure 2 was derived by Imamura and Hoffmann[25] by symmetry arguments to correlate the MO's of planar and perpendicular forms of BP.

However, the interactions of the monomeric MO's result in a substantial decrease of the HOMO/LUMO gap, by -0.59β, so π-delocalization lowers the total energy of the corresponding B_{1u} excited configuration by $-(0.38 + 0.59)\beta$. These results suggest that the BP in its B_{1u} state has a greater propensity to be planar than in the ground state. Also, the corresponding excitation energy of BP would be expected to be considerably lower than in benzene.

In reality, however, the lowest and second lowest excited states of planar BP are B_{3g} and B_{2u} which largely consist of in- and out-of-phase combinations of second highest occupied MO (SHOMO) to LUMO and HOMO to second lowest unoccupied MO (SLUMO) excitations whose energies are only -0.29β lower than in benzene. Consequently, these states would be expected to be less sensitive to torsion than the B_{1u} state.

Similar considerations also apply to the other biaryls. However, as the size of the monomeric ring system increases, the HOMO/LUMO gap decreases, as do the inter-ring interactions between the monomeric MO's. Consequently, the $\pi \rightarrow \pi^*$ excitation energies of the dimer systems move closer to the monomeric values and the π-delocalization effects in the ground and excited states become comparable.

The Hückel energies of the highest two occupied and lowest two unoccupied π-MO's of naphthalene are also shown in Figure 2, along with the MO's of planar 2,2′-BN, with which the former correlate. As these four MO's of naphthalene are nondegenerate, the situation is formally simpler than in benzene. The B_{1u} state of naphthalene can be expected to be dominated by the HOMO → LUMO singly excited configuration, while the $1B_{2u}$ and $2B_{2u}$ states would largely consist of in- and out-of-phase combinations of the SHOMO → LUMO and HOMO → SLUMO excitations. According to experiment the energy ordering of these singlet excited states is 1^1B_{2u} (^1L_b) < 1^1B_{1u} (^1L_a) < 2^1B_{2u}, suggesting that there is strong configuration interaction between the two (near-)degenerate excitations. In planar 2,2′-BN (of C_{2v} symmetry) the lowest energy B_2 (as well as A_1) excited states would then correlate with the above B_{1u} and B_{2u} states of the naphthalenic fragments, respectively. According to the semiempirical calculations of Baraldi et al., in 2,2′-BN the lowest singlet excited states, viz., 1^1B and 2^1A, correlate with the 1^1B_{2u} (^1L_b) states of the naphthalenes. Accepting this assignment as correct, in Figure 2 the configuration built largely on the HOMO → LUMO excitation is labeled as 2^1B_2 (^1L_a). This is the state then which would be most affected by inter-ring π-delocalization and therefore the one that would most prefer to be as planar as possible.

Benzene, Biphenyl, and Naphthalene: Test Calculations. The equilibrium geometry and harmonic vibrational frequencies of biphenyl in its ground state were computed by using Hartree−Fock and DFT methods in conjunction with the 3-21G and 6-31G(d) basis sets. The analogous quantities in the lowest excited state were determined by the CIS method. The results are summarized in Table 1. All computations correctly predict the ground-state geometry to be twisted. The equilibrium torsional angles range from 50.9° to 38.4°, corresponding to the lowest (HF/3-21G) and highest (B3LYP/6-31G(d)) levels of calculations, respectively. The overall consistency of these results is regarded as acceptable. Furthermore, these torsional angles are consistent with the MP2/6-31G(d) optimized value of 46°, which had been obtained by Tsuzuki et al.[30] As inter-ring dispersion is believed to be a significant component of the torsional potential, a correlated wave function method such as MP2 is expected to be more reliable than Hartree−Fock or DFT for problems such as these. On the other hand, the inter-ring (bridging) CC distance and the low frequencies (corresponding to the torsional and other inter-ring vibrational modes) appear to be remarkably insensitive to the level of computation.

On the ground-state surface the planar (D_{2h}) and perpendicular (D_{2d}) geometries (with torsional angles of 0 and 90°) correspond to transition state structures, i.e., rotational barriers. The low torsional barriers and the apparent insensitivity of the inter-ring CC distance to the relative orientation of the phenyls are of course indicative of the low degree of interaction between the phenyl moieties, i.e., no appreciable π-electron delocalization across the rings. (The relatively large delocalization energy predicted by Hückel theory is thus an overestimate.) The twisted equilibrium geometry is probably best explained in terms of competing steric repulsions and attractive dispersive interactions, which are at their maximum and minimum values, respectively, at the planar geometry, as suggested by Tsuzuki et al.[30]

The CIS calculations predict the lowest excited state to be the $^1B_{1u}$, corresponding to D_{2h} symmetry, i.e., planar geometry. This state is dominated by the HOMO → LUMO transition, as expected on the basis of the Hückel analysis. The inter-ring CC distance is ~0.08 Å shorter than in the ground state, but at the perpendicular (90°) geometry, i.e., in the ^1E state, this distance is effectively the same as in the ground state. These geometric features are interpreted as a direct consequence of the high degree of stabilization resulting from the large π-electron delocalization that occurs in this excited state. The computed excitation energies vary approximately from 37 000 to 44 000 cm^{-1} (106.1−126.4 kcal mol^{-1}), which actually bracket the experimental value of ~40 000 cm^{-1}. Thus, deviations of ~3000 cm^{-1} from experiment may be expected for related systems such as the binaphthyls.

As noted already, according to experiment, the lowest two excited states of BP are $^1B_{3g}$ and $^1B_{2u}$ states, both of which were consistently computed to lie above the $^1B_{1u}$ state when using the CIS or TD-B3LYP methods. These states largely consist of SHOMO → LUMO and HOMO → SLUMO excitation, as indicated in Figure 2, and (inter-ring) π-electron delocalization can be expected to be less important than for the $^1B_{1u}$ state. This conjecture is supported by the geometries and frequencies that were calculated for these states (Table 1). Unconstrained geometry optimizations for these states of BP indicate, however, that the equilibrium geometries are not only twisted but further distorted as a result of strong vibronic coupling with antisym-

TABLE 1: Computed Geometric Parameters, Frequencies, and Relative Energies of Biphenyl in Its Ground and Excited States

state and geometry	calculation	ϕ (torsion), deg	R_{CC}(bridge), Å	low frequencies, cm^{-1}	ΔE,[a] kcal mol^{-1}
ground state (^1A) eq^m geom (D_2)	HF/3-21G	50.9	1.490	60, 103, 126, 310	0.0
	B3LYP/3-21G	43.3	1.489	66, 94, 122, 277	0.0
	HF/6-31G(d)	45.5	1.491	67, 105, 131, 298	0.0
	B3LYP/6-31G(d)	38.4	1.486	71, 96, 129, 271	0.0
ground state (^1A_g) planar geom (D_{2h})	HF/3-21G	0.0	1.502	96i, 107, 210, 256	3.90
	B3LYP/3-21G	0.0	1.499	79i, 97, 198, 232	2.46
	B3LYP/6-31G(d)	0.0	1.494	84i, 98, 196, 227	2.09
	MP2/cc-pVQZ//MP2/6-31G(d)[b]				2.28
ground state ($^1A_1$) perp geom (D_{2d})	HF/3-21G	90.0	1.495	46i, 105, 105, 327	0.87
	B3LYP/3-21G	90.0	1.497	44i, 96, 96, 307	1.55
	B3LYP/6-31G(d)	90.0	1.496	56i, 96, 96, 302	2.51
	MP2/cc-pVQZ//MP2/6-31G(d)[b]				2.13
excited state ($^1B_{1u}$) eq^m geom (D_{2h})	CIS/3-21G	0.0	1.404	47, 70, 141, 204	126.4
	CIS/6-31G(d)	0.0	1.409	32, 70, 132, 200	120.7
	TD-B3LYP/3-21G// CIS/3-21G	0.0			114.1
	TD-B3LYP/ 6-31G(d)//CIS/ 6-31G(d)	0.0			106.1
Excited state ($^1B_{3g}$) planar geom (D_{2h})	CIS/3-21G	0.0	1.455	55i, 86, 210, 219	144.2
Excited state ($^1B_{2u}$) planar geom (D_{2h})	CIS/3-21G	0.0	1.467	104i, 98, 165, 207	150.0
Excited state ($^1B_2$) perp geom (D_{2d})	CIS/3-21G	90.0	1.491	2692i, 154i, 95, 95	156.4

[a] Adiabatic (vibrationless) relative energies. [b] Reference 30.

TABLE 2: Lowest Electronic Excitation Energies (cm^{-1}; Including Zero Point Correction ΔE_{ZPE}) of Benzene, Biphenyl, and Naphthalene Computed via CIS, TD-B3LYP, CASSCF, and CASPT2 Levels of Theory and Comparison with Experimental Data[a]

		CIS/3-21G	TD-B3LYP/3-21G	TD-B3LYP/6-31G(d)	CASSCF[b]/6-31G(d)	CASPT2[b]/6-31G(d)	exptl	ΔE_{ZPE}/3-21G
benzene	$^1B_{2u}$	51 373	44 031	42 762[c]	48 586	35 535	39 523[d]	−1094
	$^1B_{1u}$	52 163	50 024	47 990[c]	60 105	52 791	50 009[d]	−2180
	^1E_u	68 101	57 872	56 057[c]	73 778	55 269	55 978[d]	−2388
biphenyl	$^1B_{3g}$	49 322	39 158	36 900	36 950	34 739	35 296[f]	−1116
		37 472[e]	34 650[e]	33 661[e]				
	$^1B_{2u}$	51 732	41 717	39 727	39 093	37 234	36 075[g]	−689
		39 882[e]	37 209[e]	36 488[e]				
	$^1B_{1u}$	43 283	37 678	35 515	52 235	38 357	39 680[h]	−921
		41 129[e]	37 663[e]	37 534[e]				
naphthalene	^1L_b: $^1B_{2u}$	43 803	36 502	34 936	33 384	32 326	32 020[i]	−623
	^1L_a: $^1B_{1u}$	41 740	34 426	32 503	49 110	34 834	35 910[i]	−1144

[a] Ground- and excited-state geometries and frequencies determined at HF/3-21G and CIS/3-21G levels of theory, respectively, unless otherwise indicated. [b] Active spaces: 6, 12, and 10 π-MO's with 6, 12, and 10 active electrons for benzene, biphenyl, and naphthalene, respectively. [c] Geometries determined at HF/6-31G(d) and CIS/6-31G(d) levels of theory, respectively. [d] References 47 and 48. [e] Corrected energies. See text and eqs 1−3. [f] Based on observed fundamental (36 075 cm^{-1}) for $S_0 \rightarrow {}^1B_{2u}$ transition of biphenyl-d_{10} and $^1B_{2u} - {}^1B_{3g}$ separation of 750 cm^{-1} in the solid.[18,49,50] [g] Reference 21. [h] Reference 24. [i] Reference 51.

metric combinations of the breathing modes of the benzene rings. The results of this work will be reported elsewhere.[46]

In considerable contrast with the ground state, the torsional barrier height in the $^1B_{1u}$ excited state (which correlates with $^1B_2$ in D_{2d} symmetry) is estimated to be 30 kcal mol^{-1}, which can be almost entirely attributed to the presence of the large π-electron delocalization that is maximized for the planar geometry.

With regard to the correct ordering of the lowest excited states, a similar problem to BP arises also for naphthalene, where the CIS and TD-B3LYP calculations yield the incorrect 1^1B_{1u} (^1L_a) < 1^1B_{2u} (^1L_b) < 2^1B_{2u} energy ordering of these states. In an effort to better understand these systems and to determine the level of theory needed to correctly resolve the relative energetics, a series of CASSCF and CASPT2 calculations were carried out for benzene, BP, and naphthalene, in addition to the CIS and TD-B3LYP studies. The CASSCF and CASPT2 computations, performed in conjunction with the 6-31G(d) basis, utilize full valence π-MO active spaces with all π-electrons treated as active, although in the case of naphthalene a smaller active space was also tested. The results obtained are summarized in Table 2.

In the case of benzene, the TD-B3LYP/6-31G(d) calculations yield excitation energies which are within ∼3000 cm^{-1} of the experimental values, actually outperforming CASPT2, which is regarded as the highest level of theory utilized in this work. Hashimoto et al.[52] obtained excitation energies that are in better agreement with experiment using CASSCF and multireference Møller−Plesset theory, with a larger active space as well as a larger basis set than employed in this work.

For BP, as remarked above, the CIS and TD-B3LYP calculations consistently predict the $^1B_{1u}$ state as the lowest excited state, in disagreement with experiment. While the CASSCF computations predict the correct ordering of the lowest three excited states, near-quantitative accuracy is achieved only at the CASPT2 level, especially in case of the $^1A_g \rightarrow {}^1B_{1u}$ excitation, indicating that there are substantial correlation components in the corresponding excitation energy. The equilibrium geometries and frequencies of BP in its $^1B_{3g}$ and $^1B_{2u}$ states were obtained at the CIS/3-21G level of theory, assuming D_{2h} symmetry, viz., planarity. Our preliminary calculations indicate that the energetic effects of relaxing the D_{2h} constraint are fairly small, so for the purposes of this study we used the planar geometries.

Naphthalene appears to be similar to BP in that the correct ordering of the lowest two excited states is resolved only by the application of CASSCF or CASPT2. CIS and TD-B3LYP tend to underestimate this particular excitation energy, while overestimating the others, viz., $^1A_g \rightarrow {}^1B_{2u}$ as well as $^1A_g \rightarrow {}^1B_{3g}$ in the case of BP. Our CASSCF and CASPT2 excitation

TABLE 3: Equilibrium Torsional Angles of Binaphthyls in Their Ground (S_0) and Excited (^1L_a and ^1L_b) Electronic States[a]

	this work			CS-INDO/CI			experiment
	$\phi(S_0)$[b]	$\phi(^1L_a)$[c]	$\phi(^1L_b)$[c]	$\phi(S_0)$	$\phi(^1L_a)$	$\phi(^1L_b)$	$\lvert\Delta\phi(S_{n}-S_0)\rvert$
trans-1,1′-BN	78	40 (−38)	74 (−4)[d]	60	55 (−5)	49 (−11)	∼6−12
trans-1,2′-BN	61	29 (−32)	54 (−7)	55	42 (−13)	60 (5)	
cis-1,2′-BN	119	151 (32)	128 (9)	125	138 (13)	130 (5)	18[e]
trans-2,2′-BN	41	0[f] (−41)	32 (9)	35	0 (−35)	25 (−10)	
cis-2,2′-BN	136	180 (44)	144 (8)	145	180 (35)	155 (10)	32[g]

[a] Angles in degrees. The values in parentheses are the differences in angles, $\Delta\phi(S_{n}-S_0)$, between excited and ground states. [b] B3LYP/3-21G. [c] CIS/3-21G. [d] At C_2 geometry (with Hessian index of 1). [e] Based on assignment of the lowest frequency vibration as pure torsional mode, ref 14. [f] The planar ($\phi = 0$) geometry is actually predicted to be a saddle point by the CIS/3-21G calculations with an energy that is ∼6 cm^{-1} higher than the local minimum at $\phi = 9°$. [g] Reference 13.

energies are in good accord with those computed by Matos and Roos[53] and by Hashimoto et al.[52]

To assess the effect of delocalization on the excitation energies in these biaryls, it is important that we compare the appropriate excitation energies of the given aryl and biaryl systems, i.e., excited states which correlate with each other. As indicated in Figure 2, in the case of 2,2′-BN with C_2 symmetry the $1B_2$ and $2B_2$ excited states correlate with the B_{2u} (L_b) and B_{1u} (L_a) states of naphthalene, assuming that the ordering in the former is determined by the relative energies of the excited states in naphthalene. The same analysis might be expected to apply to 1,1′-BN, as it is also of C_2 symmetry. However, as will be discussed later, the strong configuration interaction between the L_a and L_b states in 1,1′-BN makes a direct correlation with the corresponding states of naphthalene less meaningful. The lack of symmetry makes the establishment of such a correlation in 1,2′-BN less obvious, but, as demonstrated by the calculations of Baraldi et al.,[29] it can be clearly identified.

In the case of BP the B_{3g} and B_{2u} states can be shown to correlate with the B_{2u} state of benzene, while the B_{1u} state of BP correlates with the B_{1u} state of benzene. The differences in the excitation energies, e.g., $\Delta E(\text{BP}:B_{3g}) - \Delta E(\text{benzene}:B_{2\text{u}})$, may then be regarded as a measure of the delocalization of the appropriate states of BP. On the basis of the experimental excitation energies, the delocalization contribution to the energies of the B_{3g}, $B_{2\text{u}}$, and $B_{1\text{u}}$ states of BP are thus estimated as approximately −4200, −3500, and −10300 cm^{-1} respectively. This trend is qualitatively reproduced by the calculations. For example, at the TD-B3LYP/3-21G level of theory the analogous delocalization contributions are −4873, −2314, and −12350 cm^{-1}, respectively. The incorrect ordering of the computed excitation energies is thus due more to the errors in resolving the excitation energies of benzene itself with sufficient accuracy. The crucial energy separation between the B_{1u} and B_{2u} states of benzene are computed to be ∼1000 and ∼6000 cm^{-1} by CIS and TD-B3LYP, respectively, whereas the experimental value is ∼10 500 cm^{-1}. In light of these results, a justifiable empirical correction to the computed excitation energies of BP would be to add to these the error in the appropriate excitation energies of benzene. The corrected excitation energies, ΔE_{corr}, are thus defined as

$$\Delta E_{\text{corr}}(\text{BP}:B_{3g}) = \Delta E(\text{BP}:B_{3g}/\text{calcd}) + [\Delta E(\text{benzene}:B_{2u}/\text{exptl}) - \Delta E(\text{benzene}:B_{2u}/\text{calcd})] \quad (1)$$

$$\Delta E_{\text{corr}}(\text{BP}:B_{2u}) = \Delta E(\text{BP}:B_{2u}/\text{calcd}) + [\Delta E(\text{benzene}:B_{2u}/\text{exptl}) - \Delta E(\text{benzene}:B_{2u}/\text{calcd})] \quad (2)$$

$$\Delta E_{\text{corr}}(\text{BP}:B_{1u}) = \Delta E(\text{BP}:B_{1u}/\text{calcd}) + [\Delta E(\text{benzene}:B_{1u}/\text{exptl}) - \Delta E(\text{benzene}:B_{1u}/\text{calcd})] \quad (3)$$

The resulting corrected CIS and TD-B3LYP excitation energies for BP are shown in parentheses in Table 2. The ordering is now in agreement with experiment and there is an improved level of consistency among the CIS and TD-B3LYP results. Moreover, especially in the case of the TD-B3LYP energies, the corrected energies are in reasonably good agreement with experiment.

Similar problems to those encountered in the CIS and TD-DFT studies of benzene exist also in the case of naphthalene. Therefore the application of analogous corrections to the BN excitation energies is expected to be similarly useful and informative.

1,1′-, 1,2′-, and 2,2′-Binaphthyls: Quantum Chemical Studies. *Geometries.* Full details of the computed ground-state geometries of the three binaphthyl systems and naphthalene itself, obtained at the B3LYP/3-21G level of theory, are available in Table S1 of the supporting information, which also contains the computed vibrational frequencies. The intra-ring bond lengths and angles are very similar to those in naphthalene itself, as expected, given the nature of the CC σ-bond that joins the two naphthalenic moieties, which would not perturb the two subsystems to any appreciable extent. As for BP, in the ground state of any of the BN systems the relative orientation of the two naphthalenic moieties is expected to be largely determined by steric interactions. Three different types of steric interactions can be anticipated for the six cis and trans forms shown in Figure 1. These are shown schematically at the bottom of the figure and labeled as “1-2”, “1-3”, and “1-4”. The hydrogen atoms attached at these points will hinder torsion about the C−C bond with the “1-2” interaction much stronger than “1-3” and a much weaker interaction for “1-4”. With the exception of 1,1′-BN, the steric interactions for each rotamer are the same, at least at this rudimentary level. Therefore, at a simple level, one would expect the stability of the cis and trans forms to be similar for 1,2′-BN and 2,2′-BN, while in the case of 1,1′-BN the steric interactions would strongly favor the trans form.

These effects are borne out by the computations, as indicated by the data in Table 3 (as well as Table S1 of the supporting information). The computed equilibrium values of the torsional angles in 2,2′-BN (only 1−4 type steric hindrance) are 41° and 136° for the trans and cis forms, respectively, which are both more planar than 1,2′-BN (1-3 type steric hindrance) with torsional angles of 61° (trans) and 119° (cis). However, while two distinct conformers, representing cis- and trans-like conformers, were identified computationally at the B3LYP/3-21G level of theory in the case of the 1,2′- and 2,2′-BN molecules, only one was found to exist for 1,1′-BN—slightly trans of perpendicular with an angle of 78°. Interestingly, in case of 1,2′-BN, no cis conformer was predicted by HF/3-21G calculations—the single equilibrium geometry found corresponds to a trans form.

TABLE 4: Inter-ring Bridging CC Distances (R_{CC}) and Lowest Four Vibrational Frequencies in Ground (S_0) and Excited (^1L_a and ^1L_b) States of Binaphthyls Computed at B3LYP/3-21G and CIS/3-21G Levels of Theory as Indicated

	S_0 (B3LYP)		^1L_a (CIS)		^1L_b (CIS)	
	R_{CC}, Å	low frequencies, cm^{-1}	R_{CC}, Å	low frequencies, cm^{-1}	R_{CC}, Å	low frequencies, cm^{-1}
1,1′-BN	1.499	17,[a] 57, 59, 143	1.430	51,[b] 71, 72,[a] 166	1.492[c]	22,[a] 65, 66, 144
trans-1,2′-BN	1.493	29,[a] 53, 63, 143	1.426	43,[b] 70,[a] 71, 148	1.480	36,[a] 58, 67, 151
cis-1,2′-BN	1.494	33,[a] 48, 63, 146	1.425	48,[b] 57,[a] 72, 146	1.479	44,[a] 50, 65, 138
trans-2,2′-BN	1.487	35,[b] 48,[a] 62, 129	1.419	9,[d] 42,[b] 87, 114	1.470	37,[b] 52,[a] 73, 133
cis-2,2′-BN	1.487	41,[a] 44,[b] 61, 130	1.418	11,[a] 39,[b] 95, 105	1.470	45,[a] 46,[b] 68, 131

[a] Torsion. [b] Butterfly. [c] At C_2 geometry (with Hessian index of 1). [d] Anharmonic torsional 0 → 1 transition frequency.

Our CIS and TD-B3LYP calculations predict the ^1L_a states of the BNs as the lowest energy excited states. For 1,2′- and 2,2′-BN this is in disagreement with the semiempirical data,[28,29] according to which the ^1L_b states have the lower energies, as in naphthalene. Since our CIS and TD-B3LYP calculations do not resolve the correct ordering of the ^1L_a and ^1L_b states in naphthalene, we assume, at least for the time being, that the same discrepancy exists for these two BNs as well. In the case of 1,1′-BN there is consensus inasmuch as all computations identify the lowest excited state as ^1L_a.

In their ground and ^1L_a excited states 1,1′- and 2,2′-BN have C_2 symmetry; the symmetries of the L_a excited states are all B. In the ^1L_b, viz., 2^1B states, however, the equilibrium geometries obtained under C_2 constraint are not local minima on the potential energy surfaces but transition state structures, i.e., they have a Hessian index of 1. Similar problems have already been noted for the $^1B_{3g}$ and $^1B_{2u}$ states biphenyl. As in that system, for 1,1′- and 2,2′-BN the normal modes with the imaginary frequencies are antisymmetric breathing vibrations of B symmetry. The equilibrium geometries and frequencies of both *cis*- and *trans*-2,2′-BN were therefore redetermined in the reduced C_1 symmetry. The drop in energy and the changes in the torsional frequencies that result from the relaxation of the symmetry constraint are fairly small (~400 and 1700 cm^{-1} in the case of energies for the cis and trans conformers, respectively) but not negligible. The analogous calculations for 1,1′-BN were not completed, due to the very troublesome nature of the optimization process, caused by the near-degeneracy of the $L_b(+)$ and $L_b(-)$ states.

The computed ^1L_a and ^1L_b excited-state geometries and frequencies of naphthalene and of the three BNs, obtained by the CIS/3-21G method, are listed in Tables S2 and S3 of the supporting information; the computed equilibrium values of the torsional angles are listed in Table 3, while the inter-ring bridging CC distances are given in Table 4. In comparison with the ground-state geometries, all molecules are computed to be substantially more planar in their ^1L_a excited states. In fact, *cis*-2,2′-BN (in its L_a state) was computed to be planar, while a slightly nonplanar geometry (with an equilibrium torsional angle of 9°) was obtained for the trans rotamer. However, as the torsional barrier to planarity in the latter was found to be just 6 cm^{-1} high, the zero-point averaged geometry of this rotamer too is planar. In general, the equilibrium torsional angles in the ^1L_a states differ from the ground-state values by 32−44°. In addition, the inter-ring CC distances are ~0.07 Å shorter in the ^1L_a states. Indeed, in these excited states, there is a clear inverse correlation between the bridging CC distance and the planarity of the system, as inferred from the computed equilibrium torsional angles. These observations are consistent with a considerably larger degree of π-delocalization in the ^1L_a states. By contrast, the torsional angles and inter-ring CC distances in the ^1L_b states are very much closer to the corresponding ground state values, suggesting a significantly lower degree of π-delocalization in the ^1L_b states. These results are in accord with the predictions of the simple Hückel model as discussed above.

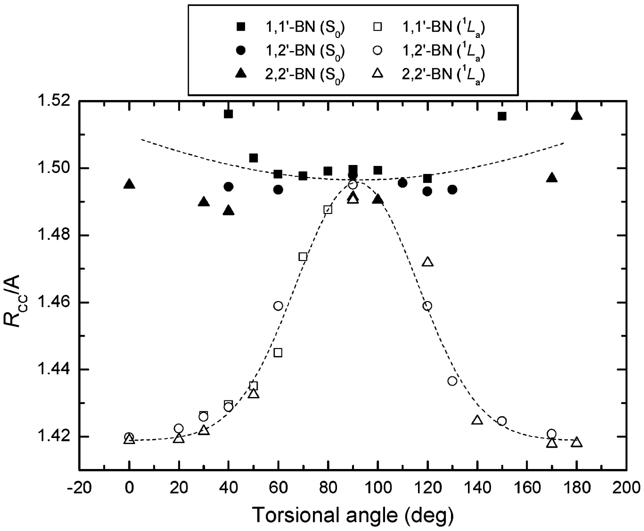

Figure 3. Correlation between the bridging CC distances and inter-ring torsions in the ground and excited states of the three binaphthyls.

On comparing the intra-ring bond lengths and angles of the three BN systems in their ^1L_a excited states with those of naphthalene in its $^1B_{1u}$ excited state, the differences are found to be more substantial than for the ground states. In particular, (a) the CC bonds flanking the bridging CC bond in the BN molecules are noticeably longer than the corresponding bonds in naphthalene, (b) the hydrogen atoms from the different naphthalenic subunits which are in close proximity to each other have been made off-planar (with respect to their parent rings), by as much as 7° in the case of 1,1′-BN, and (c) the naphthalenic rings themselves in 1,1′- and 1,2′-BN are slightly nonplanar. These distortions are consistent with the presence of substantial inter-ring π-electron delocalization, which confers some double bond character to the bridging CC bond, with a concomitant decrease of π-bonding within the rings. The increased planarity of the BN molecules which is brought about by the electronic excitation does result, however, in an increase in the steric repulsions which is then alleviated by the naphthalenic moieties themselves becoming slightly nonplanar.

As part of this work is concerned with the detailed study of the torsional potential of binaphthyls, whereby the potential is mapped out as a function of torsional angle (with all other geometric parameters allowed to fully relax), a considerable body of data has been generated that allows further exploration of the correlation between the bridging CC distance and inter-ring torsion in the BN systems in their ground and ^1L_a states. The computed points are displayed in graphical form in Figure 3. On the ground-state surfaces, while there is a definite correlation, the equilibrium inter-ring distances as a function of torsional angle vary little in comparison with what is observed for the ^1L_a excited states, where the computed distances peak sharply in the near-perpendicular region of 60−120°.

Harmonic Frequencies. The computed harmonic frequencies of naphthalene and of the three binaphthyls are given in Tables S1, S2, and S3 of the supporting information in their ground, ^1L_a, and ^1L_b states, respectively. The lowest frequencies, which mostly correspond to the inter-naphthalene torsional and wag modes, are listed in Table 4. A detailed description of the low-frequency modes and comparison with the available experimental frequencies is presented in a later section of the paper. It is worth noting at this point, however, that in the ground states of most conformers the lowest frequency corresponds to torsion with values ranging from 11 to 41 cm^{-1}. The exception is *trans*-2,2′-BN where the lowest frequency mode is an out of plane wag, which, for obvious reasons, will be referred to as a butterfly mode. Such a name is really only appropriate for systems which are near-planar, so the butterfly mode can be most readily identified for the two 2,2′-BN conformers in their ground states as well as for all ^1L_a excited states of the three BN molecules. The torsional frequencies, ranging from 11 to 72 cm^{-1}, appear to vary more than the frequencies of the wag modes such as the butterfly mode. This suggests a greater sensitivity and variability of the inter-naphthalene potential, to torsions than to other distortions. This is consistent with the notion that steric hindrance has a dominant contribution to the inter-naphthalene potential.

Since the zero-point averaged structure of *trans*-2,2′-BN is planar (which corresponds to a small barrier on the torsional potential energy surface), the torsional frequency quoted in Table 4 is the anharmonic 0 → 1 transition energy, obtained by solution of the appropriate one-dimensional Schödinger equation as described in the next section.

Torsional Potential Energy Surfaces. The potential energy surfaces of the three binaphthyls in their ground and excited ^1L_a states, computed as functions of the torsional angles, are shown in Figures 4−6, along with those obtained by the CS-INDO/S-CI method by Baraldi et al.[27−29] Our torsional potentials were calculated at the B3LYP/3-21G and CIS/3-21G levels of theory for the ground and excited states, respectively, such that for any fixed value of the torsional angle all other geometric parameters are fully optimized. (The torsional angle is defined as the C1−CC(bridge)−C2 dihedral angle, where C1 and C2 are carbon atoms flanking the CC bridge from the two naphthalenic moieties.) The resulting potential for a given molecule is therefore a minimum-energy pathway between the two distinct conformers with respect to the torsional angle as defined above. Clearly, in comparison with the ground states, the potentials are very much more sensitive to the relative orientation of the naphthalene moieties in the ^1L_a excited states. This behavior is a consequence of the greater degree of π-delocalization in these states, as discussed above, and noted already for the analogous $^1B_{1u}$ state of BP. We did not map out the corresponding torsional potentials in the ^1L_b states. However, given the relatively small π coupling in these states, as noted above, the barriers at the (near) perpendicular orientations in 1,2′- and 2,2′-BN are expected to be comparable to those in the ground states. The semiempirical calculations of Baraldi et al.[27−29] support this conjecture − their computed barriers in the ^1L_b states of 1,2′- and 2,2′-BN are approximately twice as high as in the ground states.

In response to a reviewer's query we investigated the potential effects of basis set superposition errors (BSSE) on the computed torsional potentials. This was done by the application of the counterpoise method,[54] whereby the energies of the naphthyl fragments of each BN for a range of torsional angles (ϕ) were calculated at the UHF/3-21G level in the presence of the (ghost) orbitals of the other naphthyl. The BSSE is thus quantified as

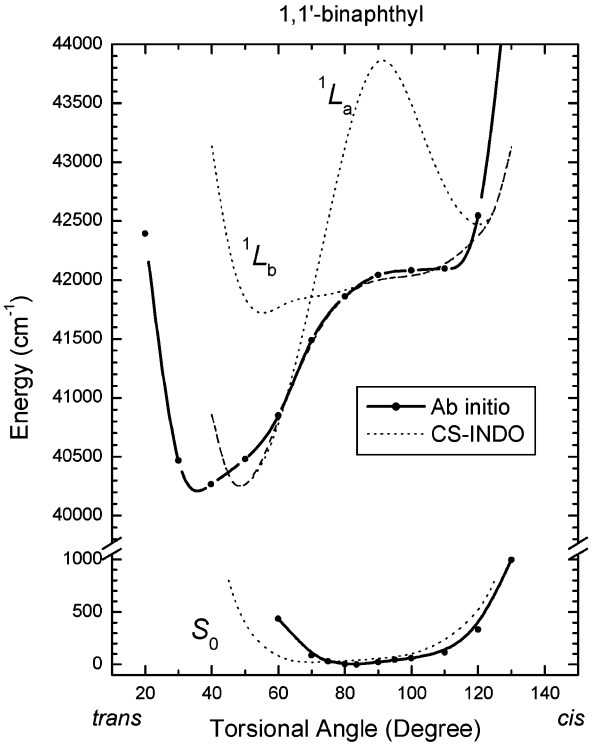

Figure 4. Torsional potential energy surfaces of 1,1′-binaphthyl in ground and excited electronic states, computed at B3LYP/3-21G and CIS/3-21G levels of theory and by CS-INDO/CI.[27] The semiempirical curve has been adjusted upward to facilitate comparison with the ab initio curve.

$$\Delta E_{\mathrm{BSSE}}(\phi) = E[\mathrm{A(B)}]_\phi - E[\mathrm{A}] + E[\mathrm{B(A)}]_\phi - E[\mathrm{B}] \quad (4)$$

where $E[\mathrm{A(B)}]_\phi$ and $E[\mathrm{A}]$ denote the energies of naphthyl A in the presence and absence of the basis functions of naphthyl B (at a given dihedral angle). The calculated BSSE's are typically around −2000 cm^{-1}. The lowest (most negative) values occur in the region of $\phi = 90°$. Thus, correcting for BSSE would actually increase the 90° barrier heights in 1,2′- and 2,2′-BN. For the latter systems the computed BSSE's vary by 449 and 519 cm^{-1} at most in the region $\phi = 0{-}90°$. The net effect on the equilibrium geometries of these two BNs is negligible, but the barriers at $\phi = 0$ would be reduced by ~100 cm^{-1} at most. For 1,1′-BN the only tangible effect of BSSE correction would be an increase in the equilibrium torsional angle in the excited state to ~50°, resulting in close agreement with the CS-INDO prediction (which is not affected by BSSE).

The ground-state potential of 1,1′-BN has a single minimum, but the well is very flat-bottomed. In light of the expected broadness of the zero-point torsional wave function, the vibrationally averaged torsional angle would be very sensitive to even minute variations in the potential, which makes the determination of any change of torsional angle on electronic excitation difficult. The excited ^1L_a state potential has a single minimum at ~40°, although, as indicated, correcting for BSSE would increase that to ~50°. There is a hint of a possible second minimum at ~115°, but our calculations produced only a point of inflection, which is a consequence of the crossing of various diabatic potential energy surfaces.[27] The existence of such regions of near-degeneracy made the computation of a relaxed adiabatic potential quite a difficult task, as noted already in the

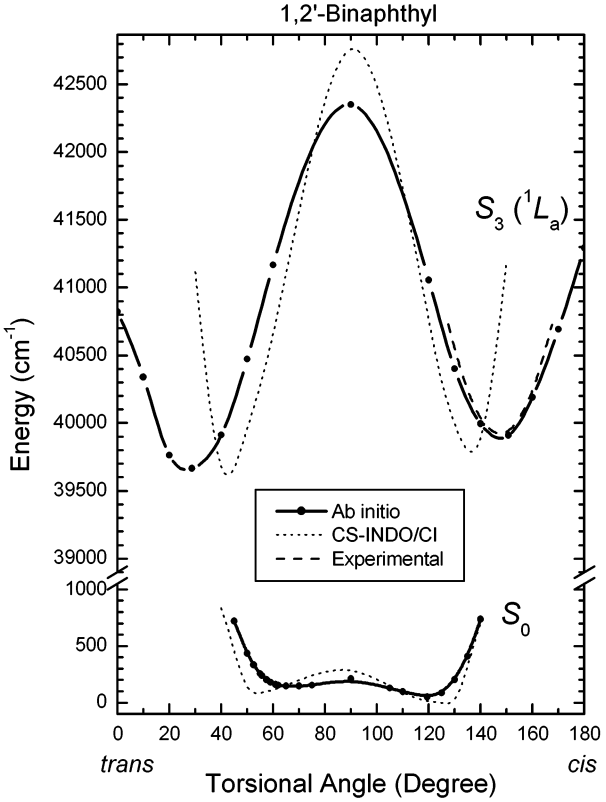

Figure 5. Torsional potential energy surfaces of 1,2′-binaphthyl in ground and ^1L_a excited electronic states, computed at B3LYP/3-21G and CIS/3-21G levels of theory and by CS-INDO/CI.[28] The semiempirical curve has been adjusted upward to facilitate comparison with the ab initio curve.

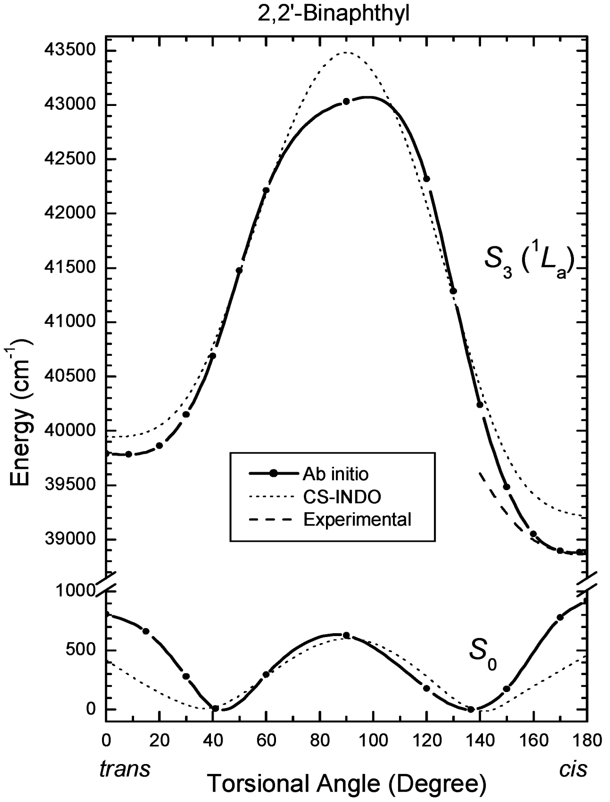

Figure 6. Torsional potential energy surfaces of 2,2′-binaphthyl in ground and ^1L_a excited electronic states, computed at B3LYP/3-21G and CIS/3-21G levels of theory and by CS-INDO/CI.[29] The semiempirical curve has been adjusted upward to facilitate comparison with the ab initio curve.

context of geometry optimization for the L_b state in C_1 symmetry. The energies at torsional angles of 20° and ≥90° were thus obtained at geometries that had been fixed at the nearest fully optimized conformations, i.e., changing only the torsional angle, as in a rigid scan. Consequently, the possible existence of a second small minimum at ~120° cannot be ruled out.

The B3LYP ground and CIS ^1L_a excited states of 1,2′-BN are both predicted to possess double-well potentials, as shown in Figure 5. As remarked above, however, the HF/3-21G calculations yielded a qualitatively different result for the ground state: a single minimum potential. The appearance of a double-well potential as a possible consequence of electron correlation is certainly an interesting and somewhat unusual effect. It is hardly surprising then that the energy barrier between cis and trans conformers, as predicted by DFT, is very low: ~60 and 160 cm^{-1} above the trans (0°) and cis (180°) conformers, respectively. While such a barrier is not sufficiently high to prevent free interconversion at room temperature, it is high enough under jet-cooled conditions (~5 K). Thus, at such low temperatures 1,2′-BN should exist largely as the cis conformer. The steep repulsive walls of the potential, as planar conformations are approached, are of course a consequence of the rapidly increasing steric repulsions between the two naphthalenic moieties, primarily due to the ortho hydrogen atoms. On the other hand, the barrier at the perpendicular form is due to the elimination of π-electron conjugation across the two naphthalenic rings, as noted already.

In the ^1L_a excited state the geometries of both *cis*- and *trans*-1,2′-BN are significantly more planar than in the ground state. Moreover, the barriers at the planar geometries are approximately half as high (1157 and 1629 cm^{-1} for the trans and cis conformers, respectively) as the one at the perpendicular geometry (2686 cm^{-1}).

The computed torsional potentials of 2,2′-BN, shown in Figure 6 are qualitatively similar to those obtained for 1,2′-BN. The main difference is near the planar geometry where the barrier to interconversion between cis and trans through this geometry is substantially smaller, as understood by 2,2′-BN only having 1-4 type steric interactions, as shown in Figure 1. According to our B3LYP calculations, in the ground state of 2,2′-BN the energy difference between the cis and trans conformers is just 9 cm^{-1}, with the barrier at the perpendicular conformation being 625 cm^{-1}, while the two barriers at the planar conformations are 805 and 920 cm^{-1} for the cis and trans conformers, respectively. On the basis of these results, we would expect *cis*- and *trans*-2,2′-BN to be present in comparable amounts under the jet-cooled experimental conditions, resulting in two distinct electronic spectra.

In the excited ^1L_a (^1B) state *cis*-2,2′-BN is planar while the trans conformer is effectively so, since the barrier at the planar conformation is only ~6 cm^{-1} (which lies 0.5 cm^{-1} below the zero-point torsional energy level). The barrier at the perpendicular geometry is 4150 cm^{-1} above the energy of the cis conformer. In comparison with the other binaphthyls, 2,2′-BN has the least amount of steric hindrance. In light of these observations, 2,2′-BN has long been predicted to have a near-planar conformation in the excited state.[5,13] Our calculations confirm this prediction in the case of the ^1L_a state, but, as the results in Table 3 show, in the ^1L_b state the equilibrium torsional angles are close to those in the ground state, i.e., the molecule is far from being planar.

TABLE 5: Lowest Energy Electronic Excitation Energies (ΔE)[a] and Oscillator Strengths (f) of 1,1′-, 1,2′-, and 2,2′-Binaphthyls Computed via CIS/3-21G and TD-B3LYP/3-21G Levels of Theory and Comparison with Semiempirical and Experimental Data

		CIS/3-21G		TD-B3L YP/3-21G		CS-INDO/CI			
		ΔE, cm^{-1}	f [b]	ΔE cm^{-1}	f	ΔE[c] cm^{-1}	f [d]	exptl	$\Delta E_{ZP\ E}$/3-21G, cm^{-1}
1,1′-BN	(^1L_a: ^1B; C_2)	39 331	0.76	30 002	0.41	31 760			
								31 716	−934
	(^1L_b: ^1B; C_2)[e]	43 729	0.0015	35 961	0.0047				
						32 980	0.034		−1262
cis-1,2′-BN	(^1L_a: ^1A; C_1)	39 038	0.78	30 609	0.50				
		33 208[f]		32 093[f]		35 290	0.627	30 828	−871
	(^1L_b: ^1A; C_1)	43 240	0.006	33 887	0.097				
		31 457[f]		29 405[f]		33 440	0.006		−665
trans-1,2′-BN	(^1L_a: ^1A; C_1)	38 794	0.86	30 383	0.50				
		32 964[f]		31 867[f]		35 290	0.503		−870
	(^1L_b: ^1A; C_1)	43 210	0.014	34 158	0.047				
		31 427[f]		29 676[f]		33 440	0.033		−647
cis-2,2′-BN	(^1L_a: $^1B_2$; C_{2v})	38 016	0.76	30 559	0.51				
		32 186[f]		32 043[f]		34 870	0.417	30 060	−864
	(^1L_b: ^1A; C_1)	42 326	0.0004	33 452	0.0082				
		30 543[f]		28 970[f]		32 670	0.042		−651
trans-2,2-BN	(^1L_a: ^1B; C_2)	38 818	1.13	31 804	0.91				
		32 988[f]		33 288[f]		35 670	0.707		−910
	(^1L_b: ^1A; C_1)	42 282	0.0001	33 034	0.021				
		30 499[f]		28 552[f]		33 160	0.044		−648

[a] Including zero point correction ΔE_{ZPE}. Zero point corrections for ground and excited states computed at HF/3-21G and CIS/ 3-21G levels of theory, respectively. [b] Evaluated at excited state (CIS/3-21G) geometries. [c] Adiabatic excitation energies, as inferred from the figures in refs 27−29. [d] Evaluated at ground-state equilibrium geometries, refs 27−29. [e] At C_2 geometry (with Hessian index of 1). [f] Corrected energies. See text and eqs 1−3.

Torsional Energy Levels. Utilizing the torsional potential surface, solution of the appropriate one-dimensional Schrödinger equation (by the generalized finite element method) yields torsional energy levels which reflect the anharmonic nature of the (one-dimensional) torsional potential. Provided the coupling to other modes is not strong, the resulting torsional energies can be meaningfully compared with observed torsional progressions.

For the ^1L_a excited states of *cis*- and *trans*-2,2′-BN the computed energy spacings show a monotonic increase with the torsional quantum number in both conformers, i.e., negative anharmonicity, in reasonable agreement with experiment, especially in the low-frequency region, below $\sim v = 12$. In the region of high torsional quanta the observed spacings become more uniform, corresponding to more nearly harmonic behavior.

By contrast, in 1,2′-BN the calculated torsional progressions in both cis and trans conformers of the ^1L_a excited state were found to be almost completely harmonic, with a near-constant spacing of ~51 cm^{-1}.

The pattern of torsional energy levels obtained for 1,1′-BN in its ^1L_a excited state appears to be quite harmonic also. Up until $v = \sim 20$ the spacing is ~52.5 cm^{-1}. Further up a small positive anharmonicity is evident, which reduces the spacing to ~30 cm^{-1} at $v = 42$. The purely torsional frequency of ~52.5 cm^{-1} is lower than the normal-mode frequency of 72 cm^{-1}, probably because the latter includes contributions from other modes.

Excitation Energies and Oscillator Strengths. The computed excitation energies and oscillator strengths for the binaphthyls are summarized in Table 5. The CIS excitation energies are typically ~9000 cm^{-1} higher than those obtained by the TD-B3LYP method. Zero-point vibrational corrections range from ~650−900 cm^{-1}, except for the excitation to the ^1L_b state of 1,1′-BN, where the equilibrium geometry (in C_2 symmetry) does not represent a local minimum on the potential energy surface, as discussed already. Since the CIS and TD-B3LYP calculations substantially overestimate the energy of the ^1L_b state in naphthalene in comparison with the ^1L_a state, we applied the same type of empirical corrections to the excitation energies of 1,2′- and 2,2′-BNs as for biphenyl, which are given by eqs 1−3. For the BNs the corrections are simply the differences between the observed and computed $S_0 \rightarrow {}^1L_a$ and $S_0 \rightarrow {}^1L_b$ excitation energies of naphthalene. One immediate effect of these corrections is that the differences between the CIS and TD-B3LYP excitations have been reduced to ~2000 cm^{-1} or less. The validity of such a correction is questionable, however, in the case of 1,1′-BN, where the strict correlation of the L_a and L_b states of naphthalene and 1,1′-BN may not hold, given the large degree of configurational mixing that exists in this system, as demonstrated by Baraldi.[27]

The $S_0 \rightarrow {}^1L_a$ excitation energies are predicted to be considerably lower in the binaphthyls than in naphthalene, by ~2400−3700 cm^{-1} at the CIS level, and by up to ~4400 cm^{-1} at the TD-B3LYP level of theory. In the case of the $S_0 \rightarrow {}^1L_b$ excitations of 1,2′- and 2,2′-BN the CIS differences between the BNs and naphthalene are considerably smaller at ~560−1520 cm^{-1}, while the TD-B3LYP shifts are comparable with what had been obtained for the $S_0 \rightarrow {}^1L_a$ excitations. Using the terminology of the excitonic model, it appears that at the CIS level the coupling between the localized $S_0 \rightarrow {}^1L_b$ excitations on the two naphthalene moieties is very small and the computed excitation energy in essence corresponds to the excitation of just one naphthalene. This explains why symmetry breaking occurs for 1,1′-and 2,2′-BN, resulting in systems where the geometry of one naphthalene moiety is essentially that of naphthalene in the ^1L_b excited state, while the other's geometry is close to that of naphthalene in its ground state. The interring coupling is predicted to be considerably stronger by the TD-B3LYP calculations, as indicated by the larger difference in the excitation energies of the BNs and naphthalene, which suggests the possibility that the symmetry breaking could be an artifact of the CIS computations. We note, however, that the TD-B3LYP excitation energies of cis and *trans*-2,2′−BN in the reduced C_1 symmetry are still lower, by 1694 and 386 cm^{-1}, respectively, than their counterparts in C_2 symmetry.

While both CIS and TD-B3LYP predict the ^1L_a excited states to have lower energies than the ^1L_b states in the BNs, the application of the empirical correction, so as to correct for the error in $^1L_a - {}^1L_b$ energy differences, switches the order, so that with the exception of 1,1′-BN, the ^1L_b states would lie ~3000 cm^{-1} lower than the ^1L_a states, in qualitative agreement with the CS-INDO/CI results. Although it cannot be ruled out that the ^1L_a states might actually be the lowest excited states, it seems unlikely on the basis of the results obtained in this work. Unfortunately, these systems are too large for CASPT2 calculations with at least the 6-31G(d) basis on the computers available for this work. Nevertheless, we were able to complete one such calculation for *cis*-2,2′-BN in C_{2v} symmetry at the CIS/ 3-21G equilibrium geometry, with 12 active π-electrons in an active space of 12 π-MO's. (The analogous CASPT2 calculation on naphthalene, with six electrons in six active π-MO's, yielded 31 671 and 33 784 cm^{-1} for the $S_0 \rightarrow {}^1L_b$ and $S_0 \rightarrow {}^1L_a$ excitation energies, which are in good agreement with CASPT2 results listed in Table 2 (with 10 active electrons in 10 active π-MO's). In the case of *cis*-2,2′-BN the CASPT2/6-31G(d) calculations have yielded adiabatic excitation energies of 28 913 and 32 731 cm^{-1} for the $S_0 \rightarrow {}^1L_b$ and $S_0 \rightarrow {}^1L_a$ transitions, respectively, in remarkably close agreement with the empirically corrected TD-B3LYP/3-21G results.

A major difference between the $S_0 \rightarrow {}^1L_a$, ^1L_b transitions is that the excitations to these two states have very different oscillator strengths, as the data in Table 5 demonstrate. At the TD-B3LYP level the computed oscillator strengths range from 0.41 to 0.91 for the $S_0 \rightarrow {}^1L_a$ transitions, but are 1−2 orders of magnitude lower for the $S_0 \rightarrow {}^1L_b$ excitations, in good accord with the CS-INDO/CI results.[27,28]

Comparison with Experiment. The electronic spectra of all three BN isomers have been measured experimentally under a variety of conditions, including solution, cryogenic matrix, and gas phase in supersonic jet.[1,14] The presence of two isomers, several low-lying electronic states and very low-frequency vibrations complicated the interpretation of the experiments. Comparison of the results of this work should help to clarify some of the questions that arose and indeed was one of the motivating factors for carrying out this study. Each BN isomer has its own characteristic set of unresolved issues and so each isomer will be discussed in turn.

2,2′-binaphthyl. The gas-phase spectrum of jet-cooled 2,2′-BN shows one pronounced progression, assigned as the torsional vibration, built on a variety of other vibronic transitions. The spectrum was interpreted as arising from the S_1 (^1L_b, ^1B) $\leftarrow S_0$ transition. Detailed analysis of the frequency pattern and intensity distribution of the torsional progression led to the conclusion that only one of the cis and trans isomers contributed to the spectrum. The previous semiempirical calculations placed the equilibrium structure of both isomers at the same energy in both ground and excited state (see Figure 6); consequently, it could not be determined unambiguously which isomer gave rise to the observed spectrum.

The present calculations again place the relative energy of the cis and trans isomers in the ground state at almost identical energies (see Figure 6). The barrier for interconversion between cis- and translike isomers is about 600 cm^{-1} through 90°. Therefore the barrier is sufficiently low, so that both conformations would exist in almost equal abundance in the room temperature vapor. As the vapor cools in a supersonic expansion, both isomers will be trapped in their respective wells, leading to almost equal populations even at very low temperature in the jet.

Several aspects of our calculations lead us to question the assumption that the experimental spectrum arises from the S_1(^1L_b) $\leftarrow S_0$ transition. Unfortunately, the estimated potential errors in our calculated 0−0 excitation energies (~3000 cm^{-1}) are too large to allow this question to be settled unequivocally. However, the oscillator strength is very weak for the $S_1 \leftarrow S_0$ transition but significant for the S_3(^1L_a) $\leftarrow S_0$ transition. Additionally, the reassignment of the experimental spectrum as $S_3 \leftarrow S_0$ provides an explanation as to why a contribution from only one rotamer was found. The calculated equilibrium energies of the cis and trans isomers in the S_3 excited state differ by about 1300 cm^{-1}, with the cis having the lower energy. The $S_3 - S_0$ transition in the *trans*-2,2′-BN molecule should therefore lie 1300 cm^{-1} above the cis origin. Consequently, the spectrum from the trans isomer would be lost in the higher lying congested vibronic structure of the cis spectrum. It is even possible that the unassigned complex structure lying 1650 cm^{-1} above the 0−0 transition in the experiment might be due to the $S_3 \leftarrow S_0$ transition in the trans rotamer. Further consequences of the reassignment are discussed below in some detail.

The matrix spectrum of 2,2′-BN was also been published by Del Riccio et al.[13] A 0−0 transition in the matrix of 28 459 cm^{-1} was assigned to the $S_1 \leftarrow S_0$ transition. The unusually large matrix shift from the gas phase (≈1500 cm^{-1}) was noted by the authors and rationalized by assigning the gas-phase transition to being a false origin. On the basis of the current work we now propose that the matrix and gas-phase spectra arose from two different transitions, with the matrix being the $S_1 \leftarrow S_0$ and the gas phase $S_3 \leftarrow S_0$. The resulting ~1500 cm^{-1} difference between the S_1 and S_3 states is in reasonable agreement with our CIS and TD-B3LYP as well as the semiempirical estimates, even given that there will be a matrix shift of a few hundred wavenumbers in the experimental S_1 value.

Several low-frequency vibrations were identified in the *cis*-2,2′-BN spectrum,[13] with frequencies of 31, 131, 140, and 200 cm^{-1}. The lowest eight vibrational frequencies for the excited state of *cis*-2,2′-BN are tabulated in Table 6. We have animated all the low-frequency modes using GAUSSVIEW and labeled them as simply as possible. The lowest frequency mode is distinctly the torsion, as assigned experimentally. The calculated harmonic frequency is significantly lower than the reported experimental frequency; however, the vibration is very anharmonic. The spacings between consecutive torsional levels, as obtained by solving the one-dimensional Schrödinger equation for the computed torsional potential, are 17, 23, 25, 27, and 29 cm^{-1} for the first five transitions, gradually increasing to 36 cm^{-1} at $v = 15$ and to 43 cm^{-1} at $v = 45$. These values are in acceptable agreement with the reported experimental torsional frequency of 31 cm^{-1}, which in fact is the asymptotic value at high v. However, the distribution of the computed Franck−Condon factors with v, which is effectively Gaussian, is spread over ~35 transitions, with the maximum at $v = 46$. By contrast, the observed torsional progressions consist of ~25 peaks with the maximum at $v = 18$. The obvious explanation for the apparent discrepancy is that it is the consequence of the computations having overestimated the difference between the equilibrium torsional angles of the excited and ground states. The computed and experimentally derived values are 44° and 32°, respectively. A series of test calculations using harmonic potentials have confirmed that such a change in geometries does

TABLE 6: Calculated and Observed Low-Frequency Vibrations in the Excited ^1L_a States of All Three BN Isomers

molecule, symmetry	calcd freq/ $\mathrm{cm^{-1}}$	symmetry	description[a]	exptl freq, $\mathrm{cm^{-1}}$
2,2′-BN (cis), ^1B (C_2)	11	a	torsion	31[b]
	39	b	o.p. sym bend (butterfly)	not obsd
	95	a	o.p. asym bend[c]	131
	105	a	i.p. sym bend[c]	140
	199	b	naphthalene ring twist	not obsd
	205	a	naphthalene ring twist	not obsd
	218	b	i.p. asym bend	not obsd
	267	a	C−C stretch	200
1,2′-BN (cis), ^1A (C_1)	48	a	o.p. bend (butterfly)	35.1
	57	a	torsion + scissors[c]	53.5
	72	a	scissors + torsion[c]	60.6
	146	a	o.p. bend (butterfly) + naphthalene twist	138.1
	192	a	naphthalene ring deformation	not obsd
	193	a	naphthalene ring twist	not obsd
1,1′-BN (trans), ^1B (C_2)	51	a	o.p. bend (butterfly)	30
	71	b	i.p. sym bend (scissors)	
	72	a	torsion	
	166	a	naphthalene ring twist	
	184	b	naphthalene ring twist	
	194	a	naphthalene butterfly	

[a] The mode description refers to motion of the two naphthalene moieties with respect to each other unless indicated (o.p. = out of plane, i.p. = in plane). [b] Highly anharmonic. [c] These two modes are strongly mixed with respect to their descriptions.

give rise to a shift and broadening of the Franck−Condon envelope that have been noted above. It is also possible that the assignment of the observed peaks, determined on the basis of one-dimensional harmonic Franck−Condon analyses, is not entirely correct either. Reassignment to a range of higher v-values would obviously reduce the discrepancy between theory and experiment.

As noted already, in contrast with the planar equilibrium geometries that had been computed for the ^1L_a state of 2,2′-BN, the equilibrium torsional angles in the ^1L_b states are very much closer to those in the ground state. The planar geometries in the latter states correspond to torsional barriers, which in *cis*-2,2′-BN were computed to be approximately 900 and 400 $\mathrm{cm^{-1}}$, respectively. The $S_1 \leftarrow S_0$ transitions would therefore occur between two double-well potentials, and the vibrational fine structure would reflect the characteristic pattern of torsional eigenvalues in the $S_1(^1L_b)$ state. On the basis of our calculated torsional energies and Franck−Condon factors, we would expect to observe transitions in the range $v \approx 10$ to $v \approx 41$. These initially correspond to doubly degenerate eigenvalues lying below ~350 $\mathrm{cm^{-1}}$ with a spacing of ~40 $\mathrm{cm^{-1}}$, levels split by 0.3, 2, 8, and 16 $\mathrm{cm^{-1}}$ due to tunneling and levels above the barrier with spacings of 20−24 $\mathrm{cm^{-1}}$. The observed progressions do not display any of these characteristics and were originally assigned in terms of single-minimum potentials for both ground and excited states, which is consistent with the single-minimum ^1L_a state and the double-minimum ground state with a doubly degenerate zero point state. The same sort of analysis would apply to *trans*-2,2′-BN as well.

Most of the low-frequency vibrations in 2,2′-BN can be described predominantly as motion of the two naphthalene moieties with respect to each other (which we call the dimer modes). The six dimer modes are all reported in Table 6. Interspersed among these are two low-frequency vibrations (twists) of the naphthalene monomers themselves. The $S_3(^1B) \leftarrow S_0(^1A)$ spectrum is dipole allowed in the C_2 point group and vibrations of *a* symmetry can form progressions. The two lowest frequency *a* vibrations after the torsion are both dimer modes and correlate reasonably well with the two experimental frequencies. The next lowest experimental frequency is 200 $\mathrm{cm^{-1}}$. It is tempting to assign this vibration to the *a* symmetry naphthalene ring twist with a calculated frequency of 205 $\mathrm{cm^{-1}}$. However, we believe the 200-$\mathrm{cm^{-1}}$ vibration is more likely to be the other dimer mode, the bridging C−C stretching mode, with a calculated frequency of 267 $\mathrm{cm^{-1}}$. The bridging C−C bond length changes considerably upon electronic excitation (Table 4) and therefore should be associated with reasonable Franck−Condon intensity. The monomeric naphthalene frameworks themselves, however, change little upon electronic excitation. Therefore we expect the naphthalene twisting vibration, although of the right frequency, to be relatively inactive in the spectrum. Table 6 summarizes the correlation between the calculated and observed vibrational modes and our proposed assignments.

1,2′-Binaphthyl. In our previous work the electronic spectrum of 1,2′-BN was likewise attributed to activity in only one of the conformers and again assigned as S_1 (^1B, ^1L_b) $\leftarrow S_0$. According to our calculations, the ground state of 1,2′-BN has a very low barrier to interconversion—from trans to cis it is only 60 $\mathrm{cm^{-1}}$, while from cis to trans it is 160 $\mathrm{cm^{-1}}$ (see Figure 5). The barriers are sufficiently low that rapid interconversion both ways should occur in the room temperature vapor, but with the population in the cis conformer favored. As the temperature is lowered in the free jet expansion the cis conformer should become increasingly favored until at experimental temperatures of 5−10 K there should be a dominant population in the cis conformer. Our calculations support the conclusion that only the cis conformer contributes to the spectrum under free jet conditions, as discussed above.

We also apply similar arguments as for 2,2′-BN because the spectrum arises from the S_3 (^1B, ^1L_a) $\leftarrow S_0$ transition rather than $S_1 \leftarrow S_0$. The oscillator strength is again strong for the ^1L_a but not the ^1L_b transition. Also, as shown below, the torsional progression is much better modeled by a $S_3 \leftarrow S_0$ progression than $S_1 \leftarrow S_0$.

The spectrum showed significant Franck−Condon activity in two vibrational modes with frequencies of 35.1 and 53.5 $\mathrm{cm^{-1}}$, which were assigned previously as the torsion and dimer butterfly mode, respectively. Our calculations suggest that these assignments are actually reversed; the butterfly motion is the lower frequency vibration. Assignments of the other low-frequency vibrations are found in Table 6. As 1,2′-BN is of lower symmetry than the other two isomers, all vibrations are of *a* symmetry and hence can form progressions. A total of four low-frequency vibrations were identified in the experimental data and these all correlate well with the four lowest computed frequencies (all dimer modes).

Unlike for 2,2′-BN, analysis of the two lowest frequency progressions revealed very harmonic vibrational levels up to 10 quanta of the butterfly and 5 quanta of the torsion. A harmonic potential fit to the experimental data is shown overlaid over the ab initio (CIS) potential in Figure 5, showing good agreement between the two (supporting the assignment as $S_3 \leftarrow S_0$ as intimated above). The same harmonic fit, but with the torsion assigned as the lowest frequency mode, as in the experimental paper matches the CIS potential less well. As in the case of 2,2′-BN, the calculations appear to overestimate the difference between the equilibrium torsional angles in the excited and ground states. The effect on Franck−Condon factors is effectively the same as for 2,2′-BN. Finally, we note that the observed strongly harmonic torsional progression implies a deep torsional well, such as computed for the S_3 state, for which the torsional barrier is approximately 3 times that in the S_1 state.

1,1′-Binaphthyl. The experiments on 1,1′-BN reveal a spectroscopy and interpretation that are quite different from those of the other two isomers.[3,9] Four very short progressions were observed in the LIF spectrum of jet-cooled 1,1′-BN near the $S_1 \leftarrow S_0$ origin. About 450 cm^{-1} higher in energy, a much strong set of transitions with similar vibronic structure were identified. The interpretation of the spectrum was that only one conformation of 1,1′-BN exists in the ground state (assigned as cislike in the paper). Absorption occurs to two different conformers (cislike and translike) in the excited state. Additionally, it was proposed that the excited state is split by the interaction of the two identical naphthalene moieties, resulting in four spectra in the origin region. The higher lying intense features were assigned as being vibronically induced in the same manner as the parent naphthalene.

The current ab initio and indeed the previous semiempirical calculations support the conclusion that only one conformer exists in the ground state. However, both calculations yield very flat potentials with the trans geometry being very slightly more stable (see Figure 4), rather than the cis geometry, as assigned previously.

Other conclusions based on the observed spectra are difficult to reconcile with the ab initio results. For example, the assignment of half of the observed progressions belonging to two stable conformers in the excited state are not borne out by the calculations, which strongly suggest that the excited state should only have a stable translike conformation with the cis side of the potential being very flat. The ab initio CIS potential for 1,1′-BN is in good agreement with the semiempirical one. Although the presence of a small minimum for the cislike conformer cannot be dismissed, our calculations suggest that it would be small and not likely to support enough bound states for a torsional progression.

It is also difficult interpret the experimental torsional progressions in terms of the calculated ground- and excited-state potentials. The observed progressions are all very short, with only three−four members observed. The intensity distributions suggest two similarly shaped wells essentially vertically above each other—quite contrary to the results of our calculations, which produced a slightly skewed Gaussian envelope of Franck−Condon factors which includes 8−10 transitions with the most intense peak corresponding to $v = 30$ in the excited state. The solution to this discrepancy may lie in the interpretation of the lowest frequency vibration as the torsional frequency. Our calculations show that the two lowest frequency modes are in fact naphthalene dimer "flapping" modes with frequencies of 50 and 71 cm^{-1} (see Table 6). If the molecule was planar, these modes would be labeled out-of-plane "butterfly" and in-plane "scissors". In the almost orthogonal geometry of 1,1′-BN they are, however, better described as flapping modes with different phase combinations, although we retain the planar nomenclature in Table 6 for comparison with the other isomers. The calculated frequency of the torsion is 72 cm^{-1}. It seems reasonable, therefore, to suggest that the observed progression is in the "flapping" dimer vibration rather than torsion, as was observed in 1,2′-BN. The torsional mode might then be one of the false origins previously assigned to the cis conformer in the excited state.

Conclusions

The primary focus of this work has been the calculation and characterization of the ^1L_a electronic excited states of 1,1′-, 1,2′-, and 2,2′-binaphthyls, especially with regard to their equilibrium geometries, low-frequency vibrations, and torsional potentials, so as to assist with the interpretation of the observed LIF spectra. In the case of 1,2′- and 2,2′-BN, a high degree of consistency between theory and experiment has been demonstrated, once the observed spectra were reassigned as $S_3(^1L_a) \leftarrow S_0$. The theoretical study of the ^1L_a states has allowed the assignment and, in some cases, reassignment of the observed low-frequency torsional and out-of-plane bends of the naphthyl moieties, in particular the identification of butterfly modes. With the help of the computed torsional potentials, the nature of the excited-state equilibrium conformations associated with the observed electronic transitions was also established, viz., essentially cis for both 1,2′- and 2,2′-BN. The results of the current calculations for 1,1′-BN are at considerable variance, however, with the prevailing interpretation of the spectral data. We recommend reexamination and reassignment of the experimental data.

On a more general level, we examined the importance of π-delocalization in the ground and first excited states of the binaphthyls and biphenyl. (More detailed calculations on the latter system also helped to evaluate the validity of our computational methodology, viz., CIS and TD-DFT in conjunction with HF and DFT(B3LYP) descriptions of the ground states and utilizing the 3-21G basis set.) The results of our calculations, as well as the experimental spectroscopic data, are consistent with the predictions of qualitative MO theory, such as Hückel theory, whereby π-delocalization is significantly more important in the ^1L_a excited states (which are dominated by HOMO → LUMO excitations) than in the ground or the ^1L_b excited states. Therefore, all three binaphthyls adopt nonplanar twisted geometries in their ground and ^1L_b excited states, while in their ^1L_a excited states they are either completely planar or considerably more so than in the ground or ^1L_b states. Similar conclusions were reached for biphenyl too, which is computed to be planar in its $^1B_{1u}$ state but nonplanar in its ground as well as in its $^1B_3$ and $^1B_2$ excited states.

On comparing our results with those from the earlier semiempirical CS-INDO/CI work of Baraldi et al.,[27−29] we found a high level of consistency between the two studies.

Acknowledgment. We gratefully acknowledge the Australian Research Council and the University of Sydney for supporting this research. We also express our thanks to the Australian Partnership for Advanced Computing National Facility for access to the COMPAQ AlphaServer SC system. A.F.Z. thanks the University of Sydney for providing a Ph.D. scholarship.

Supporting Information Available: Tables S1, S2, and S3 containing geometries and vibrational frequencies of naphthalene and binaphthyls in ground and excited states. This material is available free of charge via the Internet at http://pubs.acs.org.

References and Notes

(1) Friedel, R. A.; Orchin, M.; Reggel, M. *J. Am. Chem. Soc.* **1948**, *70*, 199.

(2) Riley, M. J.; Lacey, A. R.; Sceats, M. G.; Gilbert, R. G. *Chem. Phys.* **1982**, *72*, 83.

(3) Jonkman, H. T.; Wiersma, D. A. *J. Chem. Phys.* **1984**, *81*, 1573.

(4) Layton, E. M. J. *J. Mol. Spectrosc.* **1960**, *5*, 181.

(5) Hochstrasser, R. M. *Can. J. Chem.* **1961**, *39*, 459.

(6) Post, M. F. M.; Eweg, J. K.; Langelaar, J.; Voorst, J. D. W. V.; Maten, G. T. *Chem. Phys.* **1976**, *14*, 165.

(7) Hara, Y.; Nicol, M. F. *Bull. Chem. Soc. Jpn.* **1978**, *51*, 1985.

(8) Gustav, K.; Suhnel, J.; Wild, U. P. *Chem. Phys.* **1978**, *31*, 59.

(9) Jonkman, H. T.; Wiersma, D. A. *Chem. Phys. Lett.* **1983**, *97*, 261.

(10) Lacey, A. R.; Craven, F. J. *Chem. Phys. Lett.* **1986**, *126*, 588.

(11) Tetreau, C. *J. Phys. Chem.* **1986**, *90*, 4993.

(12) Finley, J. P.; Cable, J. R. *J. Phys. Chem.* **1993**, *97*, 4595.

(13) Del Riccio, J. L.; Zhang, F.; Lacey, A. R.; Kable, S. H. *J. Phys. Chem. A* **2000**, *104*, 7442.

(14) Zhang, F.; Votava, O.; Lacey, A. R.; Kable, S. H. *J. Phys. Chem. A* **2001**, *105*, 5111.

(15) Gamba, A.; Rusconi, E.; Simonetta, M. *Tetrahedron* **1970**, *26*, 871.

(16) Drucker, R. P.; McClain, W. M. *Chem. Phys. Lett.* **1974**, *28*, 255.

(17) Dekkers, J. J.; Hoornweg, G. P.; MacLean, C.; Velthorst, N. H. *J. Mol. Spectrosc.* **1977**, *68*, 56.

(18) Murakami, J. M.; Ito, M.; Kaya, K. *J. Chem. Phys.* **1981**, *74*, 6505.

(19) Ito, M. *J. Phys. Chem.* **1987**, *91*, 517.

(20) Werst, D. W.; Brearley, A. M.; Gentry, W. R.; Barbara, P. F. *J. Am. Chem. Soc.* **1987**, *109*, 32.

(21) Takei, Y.; Yamaguchi, T.; Osamura, Y.; Fuke, K.; Kaya, K. *J. Phys. Chem.* **1988**, *92*, 577.

(22) Chakraborty, T.; Lim, E. C. *J. Chem. Phys.* **1993**, *98*, 836.

(23) Laane, J. *J. Phys. Chem. A* **2000**, *104*, 7715.

(24) Sagiv, J.; Yogev, A.; Mazur, Y. *J. Am. Chem. Soc.* **1977**, *99*, 6861.

(25) Imamura, A.; Hoffman, R. *J. Am. Chem. Soc.* **1968**, *90*, 5379.

(26) Gondo, Y. *J. Chem. Phys.* **1964**, *41*, 3928.

(27) Baraldi, I.; Ponterini, G.; Momicchioli, F. *J. Chem. Soc., Faraday Trans. 2* **1987**, *83*, 2139.

(28) Baraldi, I.; Bruni, M. C.; Caselli, M.; Ponterini, G. *J. Chem. Soc., Faraday Trans. 2* **1989**, *85*, 65.

(29) Baraldi, I. *J. Chem. Soc., Faraday Trans. 2* **1989**, *85*, 839.

(30) Tsuzuki, S.; Uchimaru, T.; Matsumura, K.; Mikami, M.; Tanabe, K. *J. Chem. Phys.* **1999**, *110*, 2858.

(31) Karpfen, A.; Choi, C. H.; Kertesz, M. *J. Phys. Chem. A* **1997**, *101*, 7426.

(32) Platt, J. R. *J. Chem. Phys*. **1949**, *17*, 484.

(33) Foresman, J. B.; Head-Gordon, M.; Pople, J. A.; Frisch, M. J. *J. Phys. Chem.* **1992**, *96*, 135.

(34) Bauernschmitt, R.; Ahlrichs, R. *Chem. Phys. Lett*. **1996**, *256*, 454.

(35) Bauernschmitt, R.; Häser, M.; Trutler, O.; Ahlrichs, R. *Chem. Phys. Lett*. **1997**, *264*, 573.

(36) Stratman, R. E.; Scuseria, G. E.; Frisch, M. J. *J. Chem. Phys*. **1998**, *109*, 8218.

(37) Tozer, D. J.; Handy, N. C. *Phys. Chem. Chem. Phys*. **2000**, *2*, 2117.

(38) Nordholm, S.; Bacskay, G. *Chem. Phys. Lett*. **1976**, *42*, 253.

(39) Roos, B. O.; Taylor, P. R.; Siegbahn, P. E. M. *Chem. Phys.* **1980**, *48*, 157.

(40) Roos, B. O. In *Ab initio Methods in Quantum Chemistry II*; Lawley, K. P., Ed.; J. Wiley & Sons Ltd.: Chichester, UK, 1987; Vol. LXIX, p 399.

(41) Andersson, K.; Malmqvist, P.-Å.; Roos, B. O.; Sadlej, A. J.; Wolinski, K. *J. Chem. Phys.* **1990**, *94*, 5483.

(42) Andersson, K.; Malmqvist, P.-Å.; Roos, B. O. *J. Chem. Phys.* **1992**, *96*, 1282.

(43) Frisch, M. J.; Trucks, G. W.; Schlegel, H. B.; Scuseria, G. E.; Robb, M. A.; Cheeseman, J. R.; Zakrzewski, V. G.; Montgomery, J. A.; Stratmann, R. E.; Burant, J. C.; Dapprich, S.; Millam, J. M.; Daniels, A. D.; Kudin, K. N.; Strain, M. C.; Farkas, O.; Tomasi, J.; Barone, V.; Cossi, M.; Cammi, R.; Mennucci, B.; Pomelli, C.; Adamo, C.; Clifford, S.; Ochterski, J.; Petersson, G. A.; Ayala, P. Y.; Cui, Q.; Morokuma, K.; Malik, D. K.; Rabuk, A. D.; Raghavachari, K.; Foresman, J. B.; Cioslowski, J.; Ortiz, J. V.; Stefanov, B. B.; Lui, G.; Liashenko, A.; Piskorz, P.; Komaromi, I.; Gomperts, R.; Martin, R. L.; Fox, D. J.; Keith, T.; Al-Laham, M. A.; Peng, C. Y.; Nanayakkara, A.; Gonzalez, C.; Challacombe, M.; Gill, P. M. W.; Johnson, B. G.; Chen, W.; Wong, M. W.; Andres, J. L.; Head-Gordon, M.; Replogle, E. S.; Pople, J. A. *Gaussian 98*, revision A.7; Gaussian, Inc.: Pittsburgh, PA, 1998.

(44) Andersson, K.; Barysz, M.; Bernhardsson, A.; Blomberg, M. R.A.; Carissan, Y.; Cooper, D. L.; Cossi, M.; Fleig, T.; Fülscher, M. P.; Gagliardi, L.; de Graaf, C.; Hess, B. A.; Karlström, G.; Lindh, R.; Malmqvist, P.-˚A.; Neogrády, P.; Olsen, J.; Roos, B. O.; Schimmelpfennig, B.; Schütz, M.; Seijo, L.; Serrano-Andrés, L.; Siegbahn, P. E. M.; Stålring, J.; Thorsteinsson, T.; Veryazov, V.; Wierzbowska, M.; Widmark, P.-O. MOLCAS Version 5.2, Lund University, Sweden, 2001.

(45) Streitwieser, A., Jr. *Molecular Orbital Theory for Organic Chemists*; Wiley: New York, 1961.

(46) Bacskay, G. B., unpublished results.

(47) Lassetre, E. N.; Skerbele, A.; Dillon, M. A.; Ross, K. J. *J. Chem. Phys*. **1968**, *48*, 5066.

(48) Hiraya, A.; Shobatake, K. *J. Chem. Phys*. **1991**, *94*, 7700.

(49) Hochstrasser, R. M.; McAlpine, R. D.; Whiteman, J. D. *J. Chem. Phys*. **1973**, *58*, 5078.

(50) Hochstrasser, R. M.; Sung, H. N. *J. Chem. Phys*. **1977**, *66*, 3265.

(51) George, G. A.; Morris, G. C. *J. Mol. Spectrosc*. **1968**, *26*, 67.

(52) Hashimoto, T.; Nakano, H.; Hirao, K. *J. Chem. Phys*. **1996**, *104*, 6244.

(53) Matos, J. M. O.; Roos, B. O. *Theor. Chim. Acta*. **1988**, *74*, 363.

(54) Boys, F. S.; Bernardi, F. *Mol. Phys.* **1970**, *19*, 553.